RSC Advances

PAPER

View Article Online
View Journal | View Issue

Cite this: *RSC Adv.*, 2026, **16**, 15062

Micro- and nano-scale topographical alterations in dental alloys after exposure to artificial saliva: a combined SEM–AFM study

Zana Jusufi Osmani, [a] Ivana Jelovica Badovinac, [b] Koray Kara, [c] Jetmire Alimani Jakupi, [d] Arianit Reka [e] and Gordana Čanadi Jurešić *[f]

This study aimed to evaluate the surface topography and chemical stability of six commonly used orthodontic archwires: nickel–titanium, gold- and rhodium-coated nickel–titanium, stainless steel, nickel-free stainless steel, cobalt–chromium–nickel, and beta-titanium under simulated intraoral conditions. Two widely applied analytical methods were used: atomic force microscopy (AFM) and scanning electron microscopy with energy-dispersive X-ray spectroscopy, complemented by additional post-processing of the obtained data. Archwires were analyzed in their untreated state and after 28 days of exposure to artificial saliva at two pH values (5.5 and 6.6). Nickel–titanium archwires showed moderate roughness and a stable nickel : titanium ratio, but were not the most resistant under all of the conditions. Coated nickel–titanium archwires showed smoother surfaces and lower element losses, indicating a protective effect of the coating. Stainless steel wires showed moderate corrosion and localized surface cracking at pH 5.5, while Ni-free stainless-steel wires were most affected by acidic conditions and exhibited pronounced degradation and high oxygen content. Cobalt–chromium–nickel archwires maintained their surface integrity better at pH 6.6, but showed selective dissolution at pH 5.5. Beta-titanium archwires exhibited localized oxidation but stable elemental composition, supporting their potential as a hypoallergenic alternative. The inclusion of three-dimensional AFM parameters allows a more comprehensive and nuanced assessment of surface morphology, capturing subtle changes that may not be apparent with conventional two-dimensional roughness analysis alone. These results emphasize the importance of material selection based on corrosion resistance and surface stability, especially for patients with acidic oral environments or metal sensitivities.

Received 1st December 2025
Accepted 8th March 2026

DOI: 10.1039/d5ra09274d

rsc.li/rsc-advances

Introduction

The aim of every orthodontic treatment is to bring the teeth into a certain position by applying ideal forces. Orthodontic wires are used as fixed appliances to exert forces on the teeth.[1,2] In view of their complex task, the materials from which they are made must also fulfil different requirements (aesthetics, friction, formability, weldability, biostability, resilience, elasticity and shape memory).[1–3] These wires are made from different materials, each with their own specifications. Thanks to recent technological advances, wires made of nickel–titanium, cobalt–chromium, beta-titanium and multi-strand stainless steel have been developed with a wide range of properties.[1,2] Nickel–titanium (NiTi) alloy is a shape memory and super elastic alloy, and the typical composition of NiTi wires comprises 50.4% nickel (Ni) and 49.6% titanium (Ti). Beta titanium—commonly abbreviated as TMA, but designated as TiMo in this paper—offers excellent torque control and weldability, but higher friction. The typical composition comprises 79% Ti, 11% molybdenum (Mo), 6% zinc (Zn) and 4% strontium (Sr). A cobalt–chromium–nickel alloy known as blue Elgiloy consists of 40% cobalt (Co), 20% chromium (Cr), 15% Ni, 15% iron (Fe), 7% Mo and 2% manganese (Mn), approximately. It is used to produce wires that are elastic, have excellent tarnish and corrosion resistance, are inexpensive and can be soldered and welded. The austenitic stainless steel 18–8 (SS) is most commonly used for the production of SS wires. 18–8 stands for a Cr and Ni content of around 18% and 8% respectively. The most important property of this type of wire is its high corrosion resistance due to the formation of a passive oxide layer. In addition, higher forces can be generated in a shorter time with these wires, as

[a]*Faculty of Medicine, University of Rijeka, Rijeka, Croatia*
[b]*Faculty of Physics and Centre for Micro- and Nanosciences and Technologies, University of Rijeka, Rijeka, Croatia*
[c]*Graphene Application and Research Center, Izmir Katip Celebi University, Izmir, Turkey*
[d]*Department of Dental Medicine, Faculty of Medical Science, University of Tetovo, Tetovo, Republic of North Macedonia*
[e]*Department of Chemistry, Faculty of Natural Sciences and Mathematics, University of Tetovo, Tetovo, Republic of North Macedonia*
[f]*Department of Medical Chemistry, Biochemistry and Clinical Chemistry, Faculty of Medicine, University of Rijeka, Rijeka, Croatia. E-mail: gordanacj@uniri.hr*

they have a lower spring back capacity and also store less energy than TiMo and NiTi wires.[1,2]

Orthodontic wires are influenced by many factors in the oral cavity. These include saliva flow, ingested liquids and food, temperature fluctuations as well as chewing and masticatory forces. Such intraoral conditions impair the functionality of orthodontic appliances and lead to changes in their microstructure, surface topography and mechanical properties.[4] Under such conditions, corrosion may occur, along with other changes affecting the integrity of orthodontic wires. Corrosion can be caused, among other factors, by metal ions released into the medium from the metallic components of orthodontic devices. It is challenging to provide a clear and unequivocal overview of the amount of released metal ions, as many factors influence both the final quantity and the types of ions released. As expected, archwires generally release the highest levels of metal ions corresponding to their nominal composition. However, more studies are revealing the presence of various contaminants – metal ions not included in the declared alloy composition. In artificial saliva, NiTi archwires predominantly release Ni^{2+}, with occasional traces of Al, Cr or Fe in cases of contamination. SS archwires release Fe, Cr, Ni, Mo, and Mn, and may also release Cu or Al depending on alloy composition. Co–Cr archwires typically release Cr, Co, and Ni, often in higher amounts than stainless steel, while TMA archwires release Ti and Mo, with occasional Fe.[5–10] Alloys such as stainless steel, cobalt–chromium and titanium resist corrosion by forming passive oxide layers. These layers act as a barrier against further chemical attack but are susceptible to mechanical damage and chemical degradation, continuously exchanging species with the environment and adjusting their thickness and composition in response to changes in potential, pH, temperature, and the presence of aggressive anions.[11] Even when intact, the passive layers can slowly dissolve in a solution – a process known as passivation – and then reform again through exposure to oxygen – a phenomenon known as repassivation. For metals that form oxide-based passive films (*e.g.*, Fe, Cr, Ti, Ni), the passivation – repassivation cycle is commonly described in the literature using simplified stoichiometric reactions.[12–14] For metal–oxide passive films such as FeO(OH) or Cr_2O_3, dissolution is generally represented as:

$$Me\text{–}O_x + 2H^+ \rightarrow Me^{2+} + H_2O,$$

which reflects the proton-assisted breakdown of the oxide structure.

Because chromium oxide films are typically used as model passive layers for stainless steel, the dissolution step is often expressed as:

$$Cr_2O_3 + 6H^+ \rightarrow 2Cr^{3+} + 3H_2O.$$

A general reaction describing oxygen-assisted repassivation is:

$2Me^{2+} + O_2 + 2H_2O \rightarrow 2MeO(OH) + 4H^+$, a mechanism consistent with classical models of passive film regrowth on transition metals. For chromium, the exact equation does not represent a fully balanced redox reaction, but rather the net stoichiometric formation of Cr_2O_3 from aqueous Cr(III) species in the presence of dissolved oxygen:

$$4Cr^{3+} + 3O_2 + 6H_2O \rightarrow 2Cr_2O_3 + 12H^+.$$

This dynamic steady state between film dissolution and reformation helps to maintain corrosion resistance. However, acidic environments (and chloride ions) can significantly accelerate the degradation of the layers.[11,15,16] Ti is particularly susceptible in such conditions as its protective oxide layer can be locally disrupted, exposing the underlying metal to corrosive attack.[16] There is a proven positive correlation between the corrosion and surface roughness of dental archwires and the release of ions in the oral environment.[16,17] In the case of Ni, as with all metals capable of forming a passive layer (such as Cu, Al, SS, Mg, and Ti alloys), increased roughness results in a greater contact area between the corrosive medium and the metal. This roughness also allows corrosive ions to become trapped in deep grooves, which act as barriers to further ingress of corrosive ions to the uncorroded metal. In contrast, smoother Ni surfaces more readily form a stable passive film.[18]

The primary goal of enhancing aesthetic properties by applying coatings to orthodontic materials has, in turn, led to significant changes in their mechanical and biological performance. Various types of coatings are used, each serving a specific functional purpose, and they can improve surface characteristics such as roughness, layer thickness, mechanical and frictional behaviour, corrosion resistance, bacterial adhesion, and overall durability.[2,19] Stable and uniform coatings can limit ion mobility and prevent surface degradation, as seen in polymerized ionic liquid systems, where a reduced content of mobile ions contributes to the formation of more stable surface films.[20] Metallic (arch)wires can be coated with tooth-coloured polymers (such as Teflon, epoxy resin, nylon and polysulfone, *etc.*) or inorganic materials (such as chromium carbide and metal rhodium (Rd)) by air spraying or electrostatic technique.[2,21,22]

It is well known that the surface topography (the surface roughness and surface morphology) of an orthodontic wire affects its mechanical properties, aesthetic appearance, corrosion behaviour, biocompatibility, release of metal ions, and the interaction of micro-organisms with dental alloys.[4,16,17] One of the techniques available for evaluating surface roughness is atomic force microscopy (AFM), a non-invasive method that provides a three-dimensional insight into the micromorphology of the wires by performing a thorough quantitative and qualitative assessment.[3,23] The real surface geometry is so complicated that a finite number of parameters cannot provide a full description. With the increased number of parameters, a more accurate description can be obtained. Roughness parameters can be calculated in either two-dimensional (single line) or three-dimensional (for an area of a surface) forms.[24] The most important parameters to characterize surface topography, used to measure the vertical characteristics of the surface deviations,

are amplitude parameters.[24,25] R_a – amplitude average height gives a good general description of height variations, R_y – maximum peak to valley roughness, P_t – maximum height of the profile, R_{sk} – skewness of the roughness profile (used to measure the symmetry of the profile about the mean line), R_{ku} – kurtosis of the roughness profile (used to describe the sharpness of the probability density of the profile) and W_a – awerage waviness are parameters used for 2D characterization of samples. For 3D characterization, root mean square (RMS) roughness (S_q), skewness of the surface texture (S_{sk}), excess kurtosis (S_{ku}), surface slope (S_{dq}) and texture aspect ratio (S_{tr}), are parameters that can provide valuable information about the surface characteristics.[24,26,27]

Most previous studies have relied on 2D parameters (R_a, R_q, R_z) to characterize archwires made of different materials, either in the as-received state or after immersion in various media (solutions that simulate intraoral conditions).[3,28–30] The situation is somewhat better for orthodontic brackets and bands, as several studies have included a wider range of surface characterization parameters, including some 3D parameters (S_q, S_{tr}, S_{dq}, S_z, S_{ku} and S_{sk}).[31,32] However, the currently available literature generally contains little such 3D data characterization parameters.

The second method used in this study is scanning electron microscopy (SEM), which provides high-resolution images with exceptional detail. By directing a focused electron beam at a sample, the SEM detects the interactions between the electrons and the surface of the sample. In most cases, this microscope is equipped with energy dispersive X-ray spectroscopy (EDX) to enable elemental analysis.[33] SEM analysis confirmed the presence of surface defects and porosity on as-received NiTi and SS archwires, although the extent of damage varied depending on the manufacturer. These materials exhibited striations, grooves, scratches and pits.[4,34] Konda *et al.* reported significant crevice corrosion on SS, NiTi and TiMo wires after 6 and/or 12 weeks of immersion in artificial saliva, with the severity of corrosion occurring in the following order: SS > TiMo > NiTi.[35] SEM changes and detailed analyses of SS orthodontic appliance components after full orthodontic treatment[36] as well as of NiTi archwires and other SS parts immersed either individually[7] or collectively[32] in artificial saliva for 4 weeks, were also investigated. Similarly, Kararia *et al.* examined both NiTi and SS archwires after completed orthodontic treatment and confirmed significant surface alterations, including deep scratches, grooves, and pronounced dark pitting corrosion.[37]

In light of numerous studies on the morphology of orthodontic materials and the variety of techniques used in such research,[2,7,28,32,35–39] this study explores six different types of archwire materials using two relatively common analytical methods, complemented by additional post-processing of the obtained data. The aim of this study was to evaluate the surface topography—specifically surface roughness and morphology—of six commonly used archwires: NiTi, Au and Rd coated NiTi, SS, Ni-free SS, cobalt–chromium–nickel (Co–Cr) and beta-titanium (TiMo) using AFM and SEM/EDX. All AFM micrographs were further processed using Gwyddion software. In addition to the standard 2D roughness parameters, relevant 3D surface parameters were also extracted. The inclusion of 3D analysis is particularly important as it allows a more comprehensive and realistic characterization of the surface morphology compared to conventional 2D parameters. This approach provides a deeper insight into morphological changes and thus closes an existing gap in the current literature. SEM/EDX was also employed at a more advanced level to investigate the chemical composition of surface layers, particularly within areas of accumulation or damage, providing further context to the observed structural alterations. Combining AFM-based 3D characterization with larger-scale SEM observations enables more accurate detection of early or subtle surface alterations and their connection to clinically relevant degradation mechanisms, offering a more comprehensive understanding than previous studies. Finally, a possible statistical correlation between surface changes and the release of metal ions was explored, based on ICP/MS measurements of ion concentrations, in an attempt to link morphological and chemical surface features with the extent of ion release.

Materials and methods

Orthodontic appliances

Six types of preformed orthodontic archwire alloys were used in this study. NiTi archwires (BioForce Sentalloy, Dentsply GAC, USA), NiTi coated with Gold and Rhodium (High Aesthetic, Dentsply GAC, USA), SS (Remanium® Ideal arch, Dentaurum, Germany), SS Ni-free alloy (Noninium® White ideal arches, Dentaurum, Germany), CoCr alloy (Elgiloy® Ideal arches, Dentaurum, Germany) and TiMo alloy (Rematitan® Special, Dentaurum, Germany). The detailed composition of all archwires is shown in Table 1.

Table 1 Chemical composition (percentage by weight of metals present) of archwires used in the study

	Element (wt%)	Ni	Fe	Ti	Cr	Mn	Mo	Rest
Type of appliance	NiTi	50.4	—	49.6	—	—	—	
	Coated-NiTi	50.4	—	49.6	—	—	—	≤0.5 μm Au and Rh
	Stainless steel	8–10.5	68–72	—	18–20	≤2.0	—	≤0.08C, ≤ 0.1 Si, ≤ 0.03 S
	Ni-free SS	≤0.2	54–63	—	16–20	16–20	1.8–2.5	≤0.1C, ≤ 1 Si, ≤ 0.05 S
	CoCr	14–16	4–6		19–21	1–3	6–8	38–42% Co, ≤ 0.1C
	TiMo (TMA)	—	—	78	—	—	11.6	≤6 Zr, ≤ 4.5 Sn

Table 2 The most important metal ions in the experimental media used in the study (in μg l^{-1} of the medium). A detailed analysis can be found in ref. 8

γ (μg l^{-1})						
pH	Type of appliance	Ni	Fe	Ti	Cr	Mn
5.5	NiTi	18.0 ± 4.7	38.7 ± 2.1	67.6 ± 0.5	3.7 ± 0.2	8.6 ± 0.1
	NiTi-coated	0.1 ± 0.0	40.2 ± 4.6	51.5 ± 2.0	4.1 ± 0.7	8.3 ± 1.3
	Stainless steel	3.0 ± 0.1	61.3 ± 6.7	49.7 ± 4.5	3.8 ± 0.4	10.4 ± 1.1
	Ni-free SS	n.d.	28.4 ± 3.7	49.7 ± 1.9	4.9 ± 0.6	13.9 ± 1.2
	CoCr	32.6 ± 0.4	55.2 ± 11.4	56.9 ± 1.0	7.2 ± 1.0	11.2 ± 0.3
	TiMo	n.d.	52.0 ± 4.8	70.7 ± 2.8	4.0 ± 0.9	10.8 ± 0.6
6.6	NiTi	33.0 ± 9.6	90.4 ± 7.2	45.5 ± 3.9	2.9 ± 0.2	10.0 ± 1.1
	NiTi-coated	0.9 ± 0.2	91.5 ± 5.5	49.5 ± 1.6	2.0 ± 0.4	9.7 ± 0.6
	Stainless steel	2.8 ± 0.2	204.4 ± 9.9	36.1 ± 1.2	2.7 ± 0.7	11.3 ± 0.3
	Ni-free SS	6.1 ± 0.3	89.7 ± 9.1	38.0 ± 2.6	2.8 ± 0.1	14.1 ± 2.0
	CoCr	6.4 ± 0.8	83.8 ± 1.4	41.3 ± 0.9	3.1 ± 0.5	9.4 ± 0.5
	TiMo	n.d.	92.2 ± 5.3	45.0 ± 4.0	2.4 ± 0.3	10.0 ± 1.4

Preparation of the artificial saliva eluates

The experimental samples of the orthodontic archwires were prepared according to the procedure described in detail in our previous publication [28]. Each alloy sample, archwire (in quintuplicate) was immersed in sterile artificial saliva prepared according to Tanny Zucci's recipe[7] for a period of 3, 7, 14 and 28 days at 37 °C with moderate agitation on a mechanical shaker (100 rpm). The eluates of the artificial saliva were analysed by Inductively Coupled Plasma – Mass Spectrometry ICP-MS and the results were published previously.[8] In this paper concentration data for five major metals (given in Table 2), expressed in μg l^{-1}, served as input for the PCA to explore variable grouping. The core of this work focuses on the analysis of wire surface topography after the entire incubation period (28 days). Wires in their original (parent) state served as controls. A total of 18 different samples were examined (6 × 3): 6 wires made of different materials, each in intact state and after the elution experiment in artificial saliva at pH 5.5 and pH 6.6. pH 5.5 was chosen because it represents the conditions of poor oral hygiene, while pH 6.6 is the typical pH value measured in the mouth.[40]

Surface morphology determination

The appearance of the metal surface of the wires used was examined using a scanning electron microscope SEM (Jeol JSM-7800F, Japan) equipped with an energy dispersive X-ray EDX spectrometer (X-Max 80, Oxford Instruments, UK) to study the elemental composition of representative samples. In SEM analysis, secondary electrons were collected with an electron beam acceleration voltage of 10 kV and a working distance of 10 mm, while in EDX analysis a beam acceleration voltage of 12 kV was used. At least two samples of each wire were examined at three surface points, with at least three additional EDX spectroscopic examinations. The results of the EDX analysis, the composition of dental alloys, can be expressed in 2 ways: weight percent (wt%) and atomic percent (at%). at% – Representing the number of atoms of each element in the alloy – provides a better prediction of the number of atoms available for release.[41] wt% for all detected metals and at% for those most relevant to each type of archwire are shown on all SEM micrographs.

The second method for examining surface roughness is AFM. Prior to imaging, samples were cleaned for several minutes by successive rinsing with ethanol and deionized water and under ultrasound (to remove all surface contaminants) and then dried with a stream of N_2. To avoid movement during scanning, the cleaned samples were securely fixed, lying flat and completely on the surface. The non-contact Nanosurf Easy Scan mode was used to minimize tip-sample interaction and potential damage during topographic data acquisition. Prior to the measurements, the AFM system was calibrated using a standard calibration grid. The scanning area was set to 10 × 10 μm. Images were acquired with sufficient resolution to identify the necessary surface features. All relevant parameters, including scan settings, tip specifications and environmental conditions, were carefully recorded to ensure reproducibility. After acquisition, the images were processed using the AFM software to reduce noise and improve contrast. All 2D and 3D measurements were performed using the analysis tools of the AFM software and Gwyddion (Czech Metrology Institute, Brno, Czech Republic) according to the procedure described by Skliar and Chernyshev.[42] The terminology and definitions applied in this research follow the guidelines set out in ISO standards, specifically ISO 4287 and ISO 25187.[26,27] During 2D analysis in Gwyddion software, each AFM scan was processed along at least 15 profile lines in the *x*-direction and 15 in the *y*-direction. These line profiles were used to extract standard 2D roughness parameters (R_a, R_q, R_z, R_{sk}, R_{ku} and P_t). For 3D analysis, surface parameters such as S_q, S_{dq}, S_{ku}, S_{sk} and S_{tr} were directly obtained from the Gwyddion software, based on the entire scanned area.

Statistical analysis

Principal component analysis (PCA) was used to determine the possible correlation between the results of the most important released metal ions (Fe, Ni, Co, Mn, Ti) and the results of the AFM parameters (R_a, R_y, R_{sk}, R_{ku}, W_a, P_t, S_q, S_{tr}, S_{dq}, S_{sk}, S_{ku}). The Statistica software system (version 13.4.04; Tibco Software Inc, Palo Alto, CA) was used for this purpose.

Results

Surface characterization by atomic force microscopy (AFM)

NiTi orthodontic archwires. NiTi alloy (Fig. 1), with equimolar content of Ni and Ti, average R_a of the untreated sample 16 nm and maximum peak-to-valley roughness ($R_y = R_{max}$) 98 nm, with a kurtosis reflecting the normal Gaussian distribution of height (R_{ku} 3.3) and a skewness of −0.05 slightly above the mean plane, indicating that there were more peaks than valleys or that they were equal in quantity. pH 6.6 leaded to greater changes in the parameters tested compared to pH 5.5 (lower average roughness, waviness and height of the profile). In the 3D profile, the pH 6.6 profile appears to be smoothed, but the biggest change was in the excess kurtosis (S_{ku}), as the distribution of peaks around the centre plane was more uneven and asymmetrical.

Au and Rd coated NiTi archwires. It appears that the coating smoothed the surface of a NiTi archwire coated with gold (Au) and Rd (Fig. 2) – in comparison between two samples (coated NiTi sample *vs.* NiTi sample), the coated one had a lower R_a, R_y and P_t value and a similar kurtosis and skewness. Similar to uncoated NiTi archwire, a pH value of 6.6 lead to greater changes than a pH value of 5.5, but in contrast to uncoated samples, the values of the treated samples were greater. In addition, the behavior of these two wires was opposite for most of the parameters determined. The changes observed in the treatment with a pH of 6.6 were characterized by more peaks ($S_{sk} < 0$), the peaks were higher (R_a, R_y, S_q) but evenly distributed (S_{sk} around 0). Photomicroscopic images (Fig. 2c) confirmed this observation.

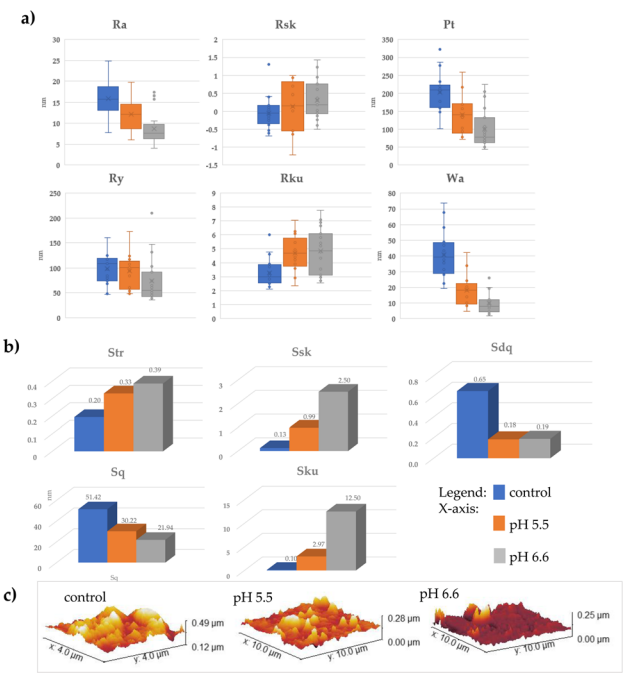

Fig. 1 Surface roughness parameters of NiTi orthodontic archwires obtained after 28-day immersion in artificial saliva, on control samples and samples exposed to two different pH values (5.5 and 6.6). (a) 2D parameters: R_a (average roughness), R_y (maximum peak-to-valley height), R_{sk} (skewness), R_{ku} (kurtosis), P_t (maximum profile height), and W_a (average waviness); (b) 3D parameters: S_{tr} (texture aspect ratio), S_q (root mean square roughness), S_{sk} (skewness), S_{ku} (kurtosis) and S_{dq} (surface slope); (c) representative AFM photomicrographs.

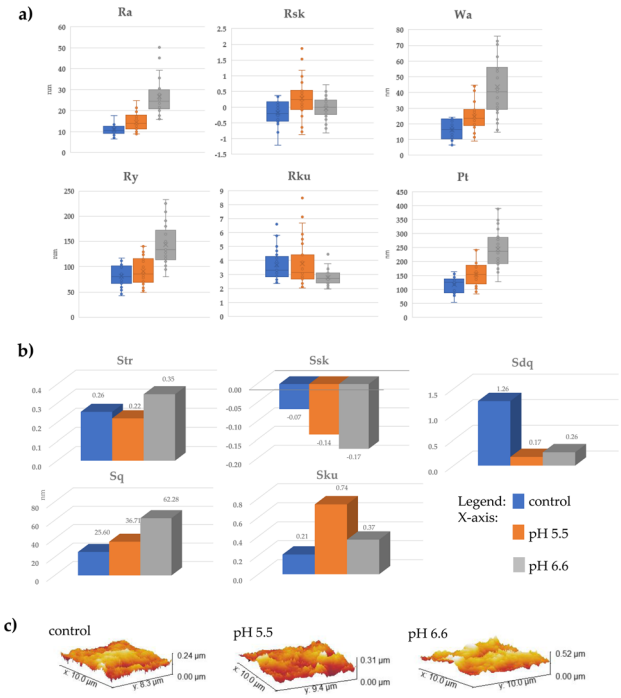

Fig. 2 Surface roughness parameters of (Au and Rd) coated NiTi archwires obtained after 28-day immersion in artificial saliva, on control samples and samples exposed to two different pH values (5.5 and 6.6). (a) 2D parameters: R_a (average roughness), R_y (maximum peak-to-valley height), R_{sk} (skewness), R_{ku} (kurtosis), P_t (maximum profile height), and W_a (average waviness); (b) 3D parameters: S_{tr} (texture aspect ratio), S_q (root mean square roughness), S_{sk} (skewness), S_{ku} (kurtosis) and S_{dq} (surface slope); (c) representative AFM photomicrographs.

SS archwires. Sample 3 (Fig. 3), a wire made from a SS alloy containing 18–20% Cr, 8–10.5% Ni, and the rest Fe, appeared to be more resistant to changes at pH 5.5 than at pH 6.6, as surface alterations were less pronounced.

The parent alloy showed a pronounced isotropy ($S_{tr} > 0.5$) with slightly more pronounced peaks (S_{ku} almost 10). When comparing the effects of the two pH values tested on the surface changes, the changes were slightly more pronounced at pH 6.6. At a pH of 5.5, as if the surface had become even smoother than that of the parent alloy, the dominance of the peaks had decreased (S_{sk} was reduced from 1.49 to 0.8), but they were still more anisotropic (S_{tr} decreased to 0.24). At a pH of 6.6, which was characterized by the highest Fe release (comparison of all samples and both pH values,[8] Table 2), the peaks presented appear to increase unevenly. This was reflected in the increase in S_q, S_{sk}, P_t and W_a. The arithmetic mean of waviness (W_a) refers to the longer-term variations in a surface profile, while P_t refers to the distance between peak and valley and captures the most significant height variations – both increased twice at a pH of 6.6. Sporadic localized increases in peak height were evident

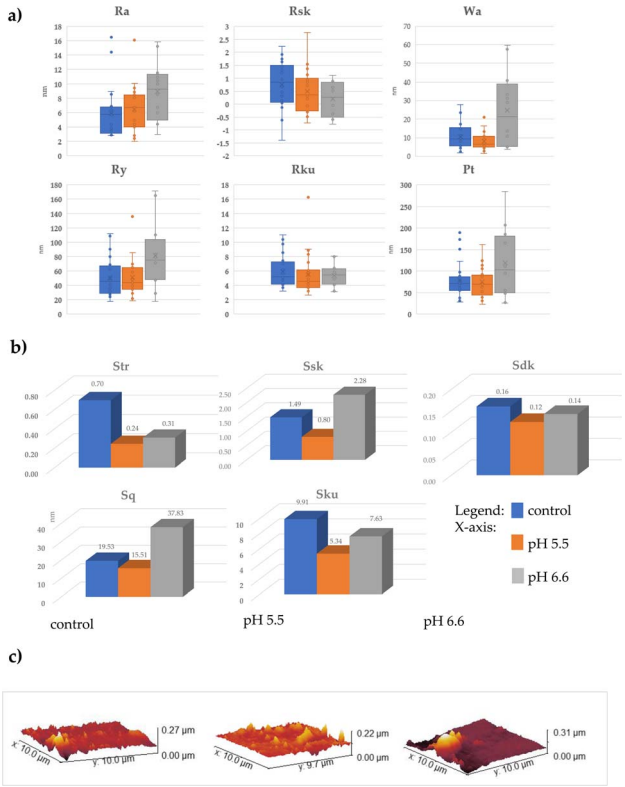

Fig. 3 Surface roughness parameters of SS archwires obtained after 28-day immersion in artificial saliva, on control samples and samples exposed to two different pH values (5.5 and 6.6). (a) 2D parameters: R_a (average roughness), R_y (maximum peak-to-valley height), R_{sk} (skewness), R_{ku} (kurtosis), P_t (maximum profile height), and W_a (average waviness); (b) 3D parameters: S_{tr} (texture aspect ratio), S_q (root mean square roughness), S_{sk} (skewness), S_{ku} (kurtosis) and S_{dq} (surface slope); (c) representative AFM photomicrographs.

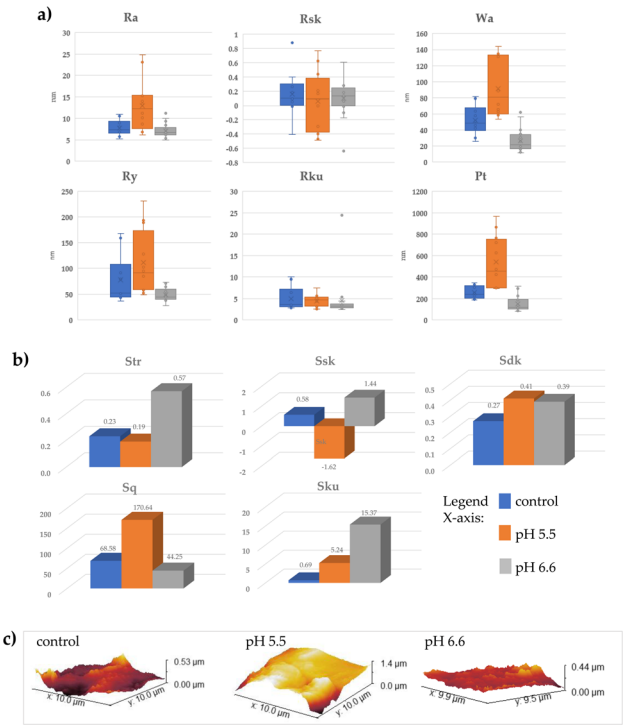

Fig. 4 Surface roughness parameters of Ni-free SS archwires obtained after 28-day immersion in artificial saliva, on control samples and samples exposed to two different pH values (5.5 and 6.6). (a) 2D parameters: R_a (average roughness), R_y (maximum peak-to-valley height), R_{sk} (skewness), R_{ku} (kurtosis), P_t (maximum profile height), and W_a (average waviness); (b) 3D parameters: S_{tr} (texture aspect ratio), S_q (root mean square roughness), S_{sk} (skewness), S_{ku} (kurtosis) and S_{dq} (surface slope); (c) representative AFM photomicrographs.

in the AFM photomicrograph at pH 6.6, indicating uneven surface morphology.

Ni-free SS archwires. Among the archwire materials tested, the Ni-free SS alloy (containing 16–20% Cr, 16–20% Mn, 1.8–2.5% Mo and the rest Fe) appeared to be the most sensitive to pH-induced changes in surface roughness parameters. This was evident from the photomicrographs, the shape of the wire and its pronounced buckling at pH 5.5 (Fig. 4).

When comparing the 2D roughness parameter R_a (arithmetic mean of roughness) across all samples of the parent alloy, Ni-free SS showed a lower roughness value than NiTi and coated NiTi and comparable values to samples SS, TiMo and CoCr. However, the 3D parameter S_q (root mean square of surface roughness) was highest for Ni-free SS, indicating that the wire was bent and its surface was highly corrugated, which was confirmed by increased W_a and P_t values. Photomicrographs of Ni-free SS reveal small sharp formations (small peaks) both in the control sample and at both pH values tested. These observations indicated that the structural changes occurred primarily within the alloy sheet itself and not on the surface. This effect was particularly pronounced at pH 5.5, where several roughness parameters reach their highest values among all samples and conditions. In particular, S_q exceeded 170 nm, while P_t and R_y also showed significant variations (P_t: 300–760 nm; R_y: 50–230 nm). In addition, the lowest value for skewness ($S_{sk} = -1.62$) indicated a surface morphology characterized by valleys rather than peaks. In contrast, the sample exposed to a pH of 6.6 was less affected. It was characterized by a higher kurtosis value (S_{ku}), which indicated the presence of peaks with a more uniform height.

Co–Cr archwires. Sample 5 (Fig. 5), Elgiloy (a CoCr alloy containing 38–42% Co, 19–21% Cr, 14–16% Ni and 6–8% Mo), was characterized by the lowest R_a value among the parent alloy samples, but showed the most pronounced changes in surface parameters at pH 6.6 compared to all other samples. At pH 5.5, the changes seem to be limited to the "growth" of existing peaks, likely resulting from surface changes caused by the highest release of Co, Ti, Ni and Fe ions. Interestingly, Ti and Fe ions were detected in the eluate, although they were not part of the nominal composition of this alloy[43] (Table 2). Exposure to a pH of 6.6 resulted in a significantly lower release of ions – about half – which was primarily due to the lower concentrations of Co and Ni. Photomicrographs of the sample at pH 6.6 shoved that the existing peaks thickened and doubled in height, as if an additional layer had formed on top of the original surface. The newly formed peaks were less uniform, as indicated by a low S_{ku} value ($S_{ku} = -0.1$).

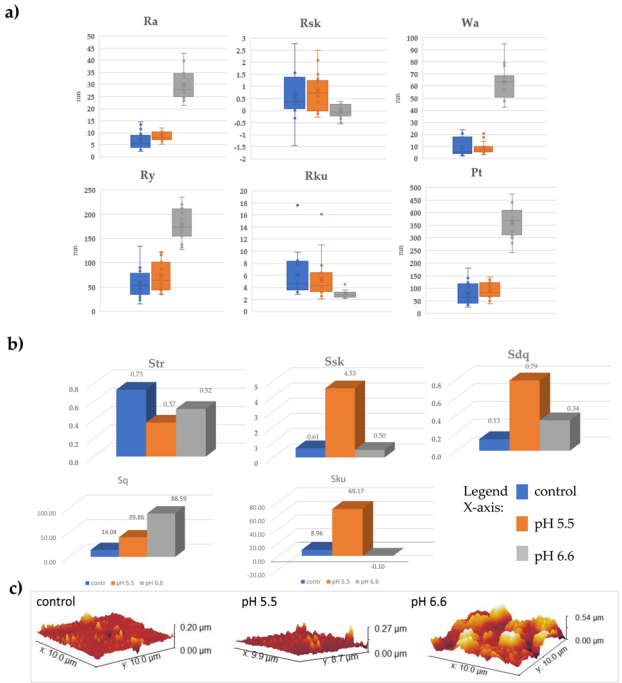

Fig. 5 Surface roughness parameters of CoCr archwires obtained after 28-day immersion in artificial saliva, on control samples and samples exposed to two different pH values (5.5 and 6.6). (a) 2D parameters: R_a (average roughness), R_y (maximum peak-to-valley height), R_{sk} (skewness), R_{ku} (kurtosis), P_t (maximum profile height), and W_a (average waviness); (b) 3D parameters: S_{tr} (texture aspect ratio), S_q (root mean square roughness), S_{sk} (skewness), S_{ku} (kurtosis) and S_{dq} (surface slope); (c) representative AFM photomicrographs.

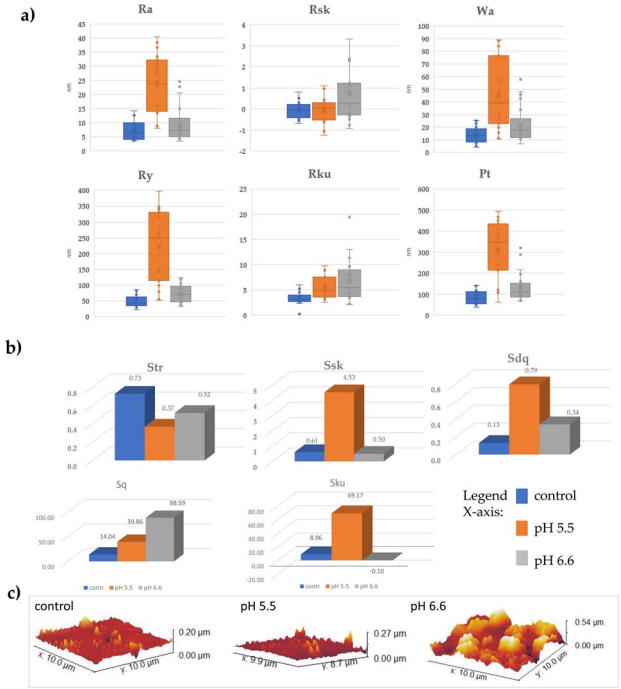

Fig. 6 Surface roughness parameters of TiMo archwires obtained after 28-day immersion in artificial saliva, on control samples and samples exposed to two different pH values (5.5 and 6.6). (a) 2D parameters: R_a (average roughness), R_y (maximum peak-to-valley height), R_{sk} (skewness), R_{ku} (kurtosis), P_t (maximum profile height), and W_a (average waviness); (b) 3D parameters: S_{tr} (texture aspect ratio), S_q (root mean square roughness), S_{sk} (skewness), S_{ku} (kurtosis) and S_{dq} (surface slope); (c) representative AFM photomicrographs.

TiMo archwires. The last sample (Fig. 6) was a Ti and Mo alloy (78% Ti and 11.5% Mo), which released similar amounts of titanium as the NiTi alloy (sample 1) at a pH of 5.5 (Table 2). Although the pattern was similar in terms of quantities and time, the surface parameters were completely different. pH 5.5 caused the strongest changes, as evident in the majority of measured parameters (R_a, W_a, R_y, P_t, S_q, S_{dq}) with changes similar to those observed in Ni-free SS, where the entire sheet appeared to be bent. The structural buckling seemed to be more pronounced at this pH level (pH 5.5), although bending of the structure was also observed in the control sample and at pH 6.6.

Surface characterization and elemental analysis by scanning electron microscopy with energy dispersive X-ray spectroscopy (SEM/EDX)

The SEM/EDX technique enables elemental analysis of a thicker portion of the surface (approximately 1 μm), emphasizing the material beneath the uppermost layer.[28,33] Despite certain limitations—such as lower accuracy for lighter elements and carbon accumulation on the surface it provides valuable insight into the surface morphology across a larger area of interest (AOI), facilitating the detection of crystalline precipitates, defects, and signs of corrosion.[43] Each wire exhibited distinct surface features, with unique defects and irregularities primarily resulting from the specific manufacturing process. These differences were already evident in the as-received condition (control sample) and become more pronounced after exposure to artificial saliva under different pH conditions.

NiTi archwires. SEM micrographs showed that the surface of the parent state of NiTi wire (Fig. 7) was smooth, evenly colored, with randomly distributed striations and darker spots, and showed no signs of damage, cracks, or corrosion products. EDX analysis indicated low oxygen content and a balanced Ni : Ti ratio, typical of well-preserved material. At pH 5.5, the surface remained structurally similar to the control, but slight changes in texture and the appearance of darker zones were observed, which could indicate initial corrosion changes. There were no major cracks or porosity; the changes were localized and microstructural, with occasional cracks. In these zones, the oxygen content was higher. At pH 6.6, the surface was slightly rougher and had minor surface irregularities. There were no deep defects, and the slight changes in surface structure resulted from oxidation processes, as confirmed by increased oxygen content. These zones with higher oxygen content were specifically highlighted in the figures by a yellow arrow. At pH 6.6, EDX analysis revealed appreciable amounts of Al along with increased oxygen content, indicating possible formation of aluminum oxide (alumina). Although this is unexpected because Al is not listed in the nominal alloy composition, this finding is not unusual. Significant amounts of Al have been

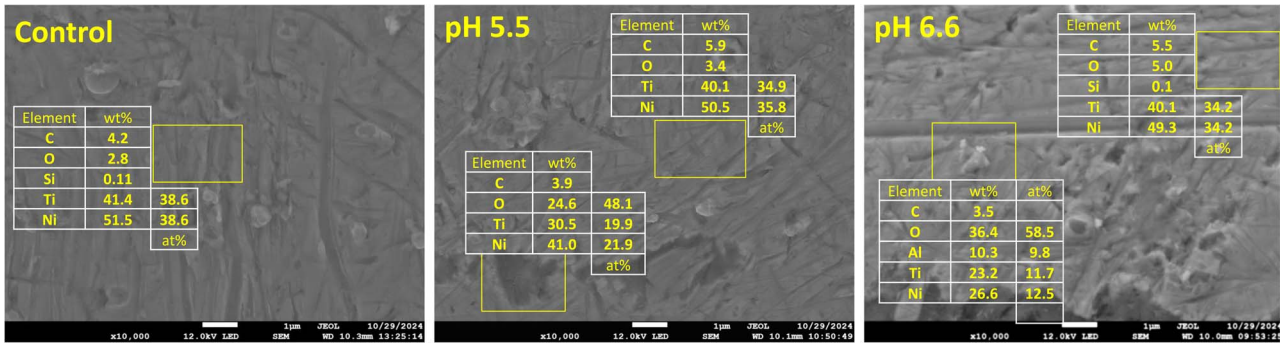

Fig. 7 Representative SEM micrographs of NiTi archwires (from left to right: control, parent sample, sample at pH 5.5 and pH 6.6).

detected in both as-received NiTi wires and in surface precipitates after exposure to artificial saliva.[7,44]

Au and Rd coated NiTi archwires. In the control sample of the coated NiTi archwire, SEM micrographs (Fig. 8) show a relatively smooth surface without major grooves or protrusions. As a result of the EDX analysis, Ti was detected among the "build-up" elements, but Ni was not observed. The element S was frequently found, which was an unusual finding. Judging by the appearance of the test samples, the coating seemed to really preserve the alloy. A pH of 5.5 appeared to be slightly more invasive as deeper groove damage was occasionally observed on the surface. Crystals of various salts can also be found on the surface of this wire at both pH values tested. In the EDX analysis, Al, Si, K, Ca and Cl ions were detected. At pH 6.6, in addition to those ions, Ni was also detected in localized regions exhibiting increased surface roughness, microcracks, and apparent structural degradation. Microcrystalline deposits of salts (NaCl and KCl) on NiTi archwire surfaces, after immersion for a certain period in either artificial saliva or *in vivo*, have been confirmed in other studies, with a significant impact on surface composition and topography.[7,45]

SS archwires. The SEM qualitative assessment of the SS archwire surface revealed clearly defined striations and localized small pits on an otherwise relatively smooth surface (Fig. 9). EDX analysis of these smooth areas reflected the nominal alloy composition. The most pronounced changes due to the tested pH values were observed in the pits and striations. At pH 5.5, the pits appeared deeper and larger, with seemingly sharper edges. EDX analysis confirmed only minor changes in elemental composition. At pH 6.6, these edges appeared less sharp. Moreover, an additional layer appears to extend across the entire surface. The amount of oxygen measured in this area was higher and suggests the formation of a protective oxide layer.

Ni-free SS archwires. In contrast to the other samples, EDX analysis showed that the parent Ni-free SS wire had a slightly different composition than specified (Fig. 10). It contained less Fe, little or no Mo, and also Ti and Au, which are not specified for this alloy (Table 1). Ti and Si were also found in treated samples – however, the content was higher at pH 6.6 than at pH 5.5. At pH 5.5, the SEM micrographs of the surface showed significant changes, including pronounced roughness, cracks, and accumulated corrosion products. Localized corrosion zones were clearly visible, the degraded layer was visible and the structure appeared rough and layered, which was probably due to the intense oxidation of metals including Fe, Mn and Cr.

The EDX analysis confirmed the increased oxygen content and the probable formation of complex oxides. At a pH of 6.6, the surface was less damaged than at a pH of 5.5, but there were also aggregated and cracked areas that could represent corroded zones. Again, the EDX analysis confirmed areas of oxidation with a higher oxygen content.

CoCr archwires. The SEM micrographs of the surface of the parent CoCr alloy sample (Fig. 11) appeared uniform and compact, with slight traces of microstructure and no evidence of cracks or corrosion changes. The low oxygen content indicated

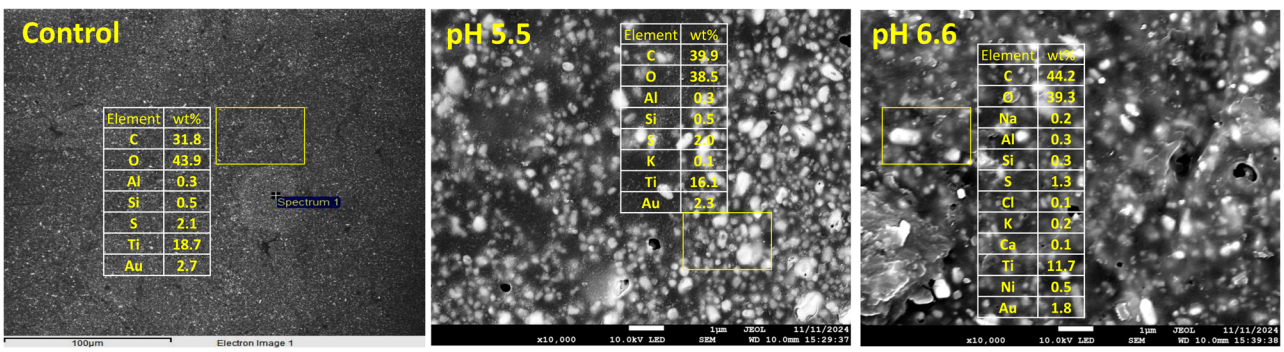

Fig. 8 Representative SEM micrographs of coated NiTi archwires (from left to right: control, parent sample, sample at pH 5.5 and pH 6.6).

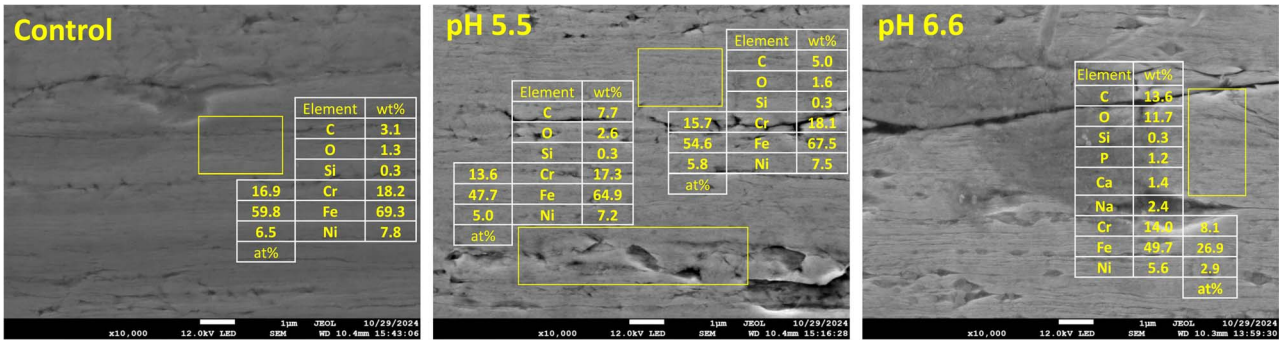

Fig. 9 Representative SEM micrographs of SS archwires (from left to right: control, parent sample, sample at pH 5.5 and pH 6.6).

a preserved protective layer with a stable Co–Cr–Ni–Fe–Mo ratio (EDX analysis). At a pH of 5.5, the surface showed localized cracks and the appearance of striations with a disturbed continuity of the passive layer, especially around the cracks. Increased oxygen content indicated oxidation, especially in the areas with cracks. The decrease in key constitutive elements might have been the result of selective dissolution of elements from the surface layer. At a pH of 6.6, the surface was relatively well preserved with only minor mechanical damage and no visible corrosion pitting. Slight unevenness and striations indicated incipient oxidation of the surface, but without deep damage.

TiMo archwire. SEM micrographs of the parent TiMo sample showed a compact, smooth, continuous surface dominated by parallel lines from processing, with no damage or porosity (Fig. 12).

EDX analysis showed the dominance of titanium, with a small amount of molybdenum; zirconium (Zr) and tin (Sn) were also present in the nominal composition (as specified, Table 1). At a pH value of 5.5, the surface exhibited localized cracks due to deep striations. The unchanged amount of oxygen indicated an intact layer without significant oxidation. However, there were localized areas of increased oxygen content and more intense oxidation, accompanied by a decrease in titanium concentration. In these areas, the alloy reacted with the formation of a thicker oxide layer. At a pH value of 6.6, the surface of this alloy was chemically more stable and had an even thicker oxide layer, which appeared to be less firmly localized.

PCA analysis

Principal Component Analysis (PCA) is a linear dimensionality reduction method that transforms a set of mutually correlated variables into a new set of mutually uncorrelated variables called principal components. The transformation is based on linear combinations of the original variables, with the first component explaining the largest portion of the total variance, the second component explaining the largest portion of the remaining variance, and so on. The aim of PCA is to identify the directions of greatest variability in the data, project the data onto those directions, and facilitate interpretation, visualization, and further analysis. The result is a reduced number of independent (orthogonal) dimensions that retain as much information as possible from the original dataset.[46] In PCA terminology, cases represent the individual objects or samples on which the variables, the measured characteristics or parameters, are recorded. In this study, the different types of orthodontic wires (NiTi, NiTi coated, SS, Ni free SS, CoCr, TiMo) in parent (control) sample and at pH 5.5 and 6.6, were treated as cases. The analyses performed (AFM parameters and the five most highly expressed metals eluted from the orthodontic appliances) were used as variables. Fig. 13 shows the values of the principal components and their contributions to the total variance.

The PCA diagram (on the left, Fig. 13) illustrates the contribution of the individual variables to the formation of the two principal components: factor 1 (36.33%) and factor 2 (21.62%), which together explain 58% of the total variance in the data set

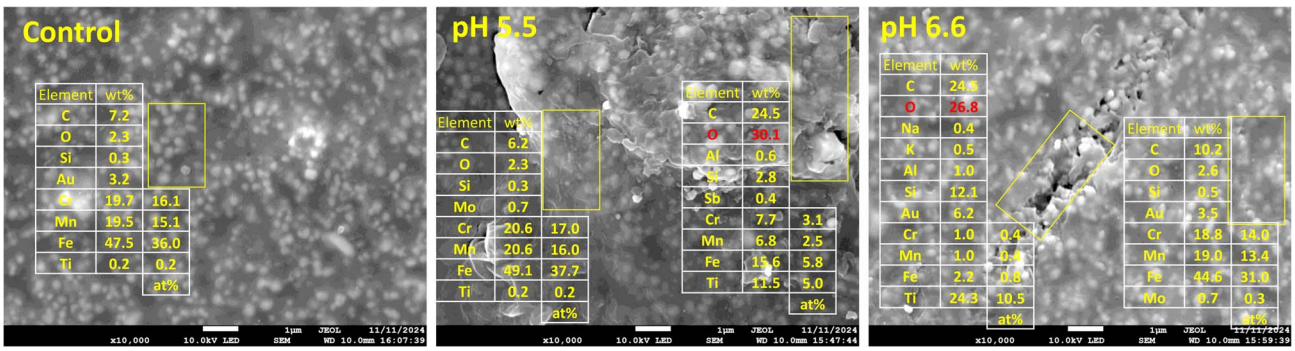

Fig. 10 Representative SEM micrographs of Ni-free SS (from left to right: control, parent sample, sample at pH 5.5 and pH 6.6).

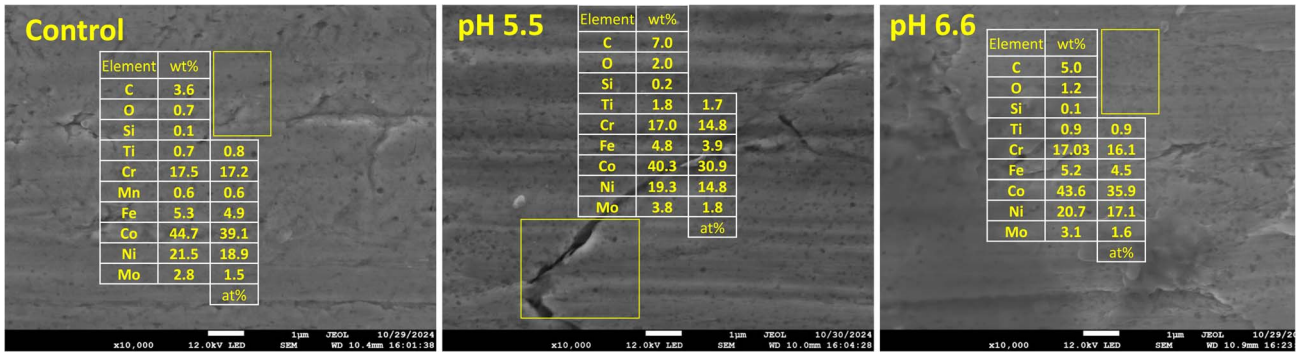

Fig. 11 Representative SEM micrographs of CoCr archwires (from left to right: control, parent sample, sample at pH 5.5 and pH 6.6).

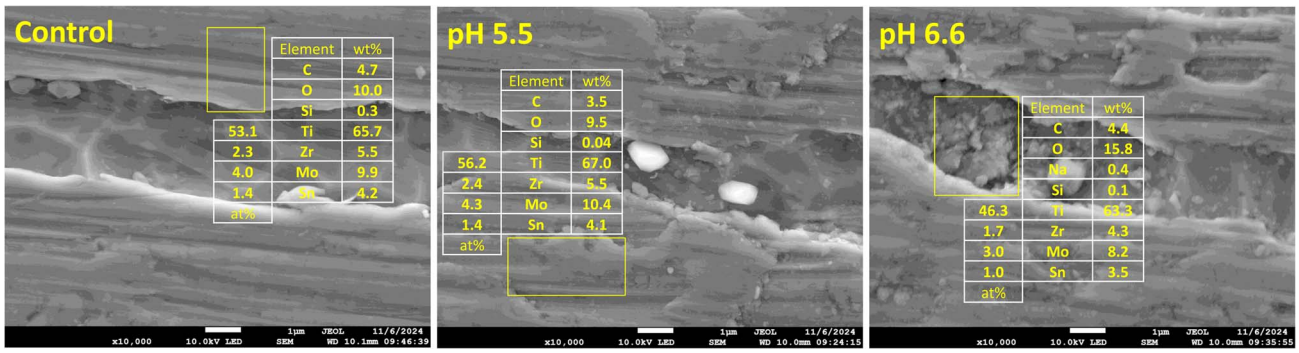

Fig. 12 Representative SEM micrographs of TiMo archwires (from left to right: control, parent sample, sample at pH 5.5 and pH 6.6).

(Table 3). The variables are represented as vectors originating from the center of the graph.

The direction of each vector indicates its correlation with the principal components, while the length of the vector reflects the strength of its influence on the differentiation of the sample. It is clear from the diagram that the variables are divided into three functional groups. The first describes the surface geometry and texture, so we can call them topographical parameters (R_{sk}, R_{ku}, S_{sk}, S_{ku}, S_{tr}), the second represents the chemical composition (Ni, Co, Fe, Mn, Ti) and the third refers to the surface performance (W_a, S_q, P_t, R_y), so we can call them mechanical parameters.

We can call factor 1 a chemical factor, as it is mainly described by changes in chemical elements, while factor 2 is

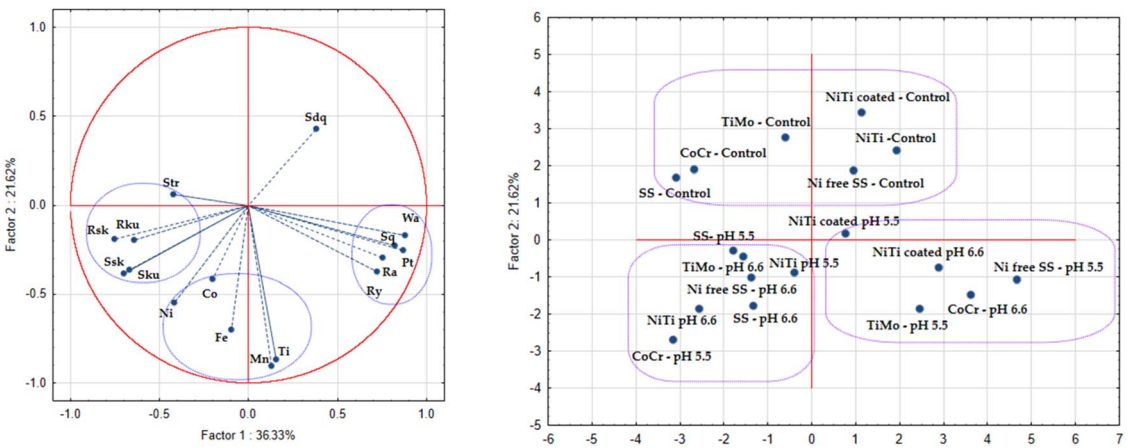

Fig. 13 Principal component analysis (PCA) applied to orthodontic archwires (NiTi, NiTi coated, steel, Ni-free SS, CoCr, TiMo, in parent sample (control) and at pH 5.5 and 6.6), five released metals (Fe, Co, Ni, Mn and Ti) and AFM parameters (R_a, R_y, R_{sk}, R_{ku}, W_a, P_t, S_q, S_{tr}, S_{dq}, S_{sk}, S_{ku}). The planes correlate components 1 and 2 (with eigenvalue 5.81 *vs.* 3.46). The left side of the figure projects the variables, while the right side shows the cases.

Table 3 Eigenvalues of correlation matrix, and related statistics of orthodontic archwires (NiTi, NiTi coated, steel, Ni-free SS, CoCr, TiMo, in parent sample (control) and at pH 5.5 and 6.6), five released metals (Fe, Co, Ni, Mn and Ti) and AFM parameters (R_a, R_y, R_{sk}, R_{ku}, W_a, P_t, S_q, S_{tr}, S_{dq}, S_{sk}, S_{ku})

Component	Eigenvalue	% Of total variance	Cumulative %
1	5.81	36.33	36.33
2	3.46	21.63	57.95
3	1.67	10.42	68.37
4	1.27	7.92	76.29
5	1.19	7.30	83.59

topographical, as the vectors of these parameters are mainly oriented towards it. The PCA scatter plot (right, Fig. 13) shows the distribution of the samples based on their surface and compositional characteristics under different conditions: control, pH 5.5 and pH 6.6. Some important observations can be made: The control samples tend to cluster together, indicating consistent baseline characteristics across all materials. All "treated" samples (eluted in AS) differ to varying degrees from the corresponding control samples, demonstrating that the elution affects the surface or chemical properties. Some of the materials used in the research (*e.g.* CoCr, TiMo, Ni-free SS) show larger shifts at two pH values used, which indicates a higher sensitivity to environmental changes. The relative positioning of the samples along factor 1 and factor 2 reflects the influence of chemical and topographical parameters respectively (as derived from the variable plot – left diagram).

The eigenvectors of the correlation matrix (in Table 4) were used to interpret the principal components. Each eigenvector reflects the contribution of the individual variables to the corresponding principal component (factor 1 to factor 5). Factor 1 is primarily determined by parameters related to macro-roughness and mechanical surface features (W_a, P_t, S_q, R_a and R_{sk} have the highest loadings). Factor 2 is dominated by the chemical elements: Mn, Ti, Fe and Ni, which have strong negative loadings. Factor 3 combines surface sharpness and chemical influences: R_{ku}, Ni, S_{dq}, Co and S_{tr} contribute the most. Factor 4 captures the directionality and height variation of the surface, suggesting a texture factor (S_{tr}, R_a, R_y and S_q). Factor 5 reflects the asymmetry of the profile and the contrast in the release of elements possibly related to specific alloy compositions (Co, Fe, S_{tr} and R_{sk}).

Table 4 Eigenvector of correlation matrix for orthodontic archwires (NiTi, NiTi coated, SS, Ni-free SS, CoCr, TiMo in parent sample (control) and at pH 5.5 and 6.6), five released metals (Fe, Co, Ni, Mn and Ti) and AFM parameters (R_a, R_y, R_{sk}, R_{ku}, W_a, P_t, S_q, S_{tr}, S_{dq}, S_{sk}, S_{ku})

Variable	Factor 1	Factor 2	Factor 3	Factor 4	Factor 5
R_a	0.314	−0.158	0.162	0.398	−0.214
R_y	0.301	−0.203	0.068	0.348	−0.227
R_{sk}	−0.313	−0.103	−0.241	−0.145	−0.332
R_{ku}	−0.268	−0.106	−0.411	−0.078	−0.089
W_a	0.365	−0.091	−0.225	−0.203	−0.037
P_t	0.361	−0.137	−0.221	−0.206	−0.100
S_{tr}	−0.176	0.033	−0.311	0.444	−0.352
S_q	0.340	−0.123	−0.267	−0.310	−0.007
S_{sk}	−0.290	−0.207	0.226	0.135	0.135
S_{ku}	−0.278	−0.195	−0.183	−0.193	0.178
S_{dq}	0.158	0.230	0.344	−0.2253	0.134
Ti	0.064	−0.466	0.035	0.0663	−0.008
Fe	−0.040	−0.377	0.010	0.2433	0.445
Mn	0.053	−0.487	−0.084	−0.0803	0.210
Co	−0.084	−0.226	0.32	−0.276	−0.566

Discussion

In the present study, the topographic surface properties of untreated orthodontic archwires and archwires placed in artificial saliva at 2 different pH values (pH 5.5 and 6.6) for 28 days were analyzed using complementary methods: AFM and SEM. AFM uses a sharp tip attached to a flexible cantilever to scan the surface, while SEM uses an electron beam for this purpose. SEM can analyze larger areas compared to AFM (several μm^2 – several mm^2 for SEM *vs.* several μm^2 – several hundred μm^2 for AFM).[3,25] SEM provides two-dimensional images of the surface, but can also provide information on the chemical composition and crystalline structure of the sample by energy dispersive X-ray spectroscopy (EDS). AFM provides three-dimensional information about surface topography and enables detailed mapping of height profiles, achieving very high resolution (down to the atomic level).[25,33]

Our AFM results (Fig. 1–6) show that, among the tested archwires in their untreated state (control samples), CoCr, SS, coated NiTi, and TiMo exhibited relatively low surface roughness, as indicated by both 2D (R_y) and 3D (S_q) parameters. In contrast, the Ni-free SS and NiTi archwires showed slightly higher roughness values. The obtained R_y values are consistent with the range reported by Uysal *et al.* in their comprehensive review, namely between 0.06 and 0.89 μm for AFM-based measurements of different NiTi alloys.[38] In their investigations, D'Antò *et al.* monitored the roughness of the wires in the untreated state. They did not have a CoCr variant, but the SS wire proved to be the least rough, while the coated NiTi wire was the roughest.[3] There are several advantages to using materials with lower surface roughness values. Such materials are considered more suitable for orthodontic applications due to reduced biofilm adhesion, lower frictional forces between wires and brackets, decreased nickel ion release, and minimized intraoral corrosion associated with wire degradation.[38] Changes in surface roughness under different pH conditions varied depending on the wire material. For coated NiTi, SS, and CoCr wires, the highest roughness was observed at pH 6.6. In contrast, Ni-free SS and TiMo wires exhibited the highest roughness at pH 5.5. Interestingly, for NiTi wire, the untreated sample showed the highest roughness, while the lowest was recorded after exposure to pH 6.6.

If all parameters analyzed for a single archwire are considered, certain similarities can be observed between the values of the individual analyzes. For example, the 2D parameters R_a, R_y, W_a and P_t show very similar trends, which are also reflected in the 3D parameter S_q. However, more pronounced differences can be

observed between the kurtosis and skewness parameters (R_{ku} and R_{sk} in 2D; S_{ku} and S_{sk} in 3D), mainly because the 3D parameters take into account the entire surface and not just a single cross-sectional profile, thus allowing a more accurate assessment of surface heterogeneity. When S_{ku} is greater than R_{ku}, this indicates that the 3D surface has more pronounced peaks and valleys than the individual 2D profiles suggest, especially when the selected profile does not pass through these extreme points (as observed for NiTi and Ni-free SS at pH 6.6 and CoCr at pH 5.5). Since the distribution of peaks is often spread over the surface, 3D analysis is better suited to capture these features than a single line profile. A similar relationship can be observed between S_{sk} and R_{sk}: while R_{sk} describes the asymmetry of the height distribution along a single profile, S_{sk} provides a more comprehensive evaluation by considering the entire surface and thus provides a more reliable indication of the prevalence of peaks or valleys in the sample. For instance, a negative S_{sk} value was obtained for a relatively smooth but fracture-prone sample (coated NiTi, Fig. 2), indicating a surface dominated by valleys.

In contrast, increased S_{sk} and S_{ku} values – alongside lower R_{sk} and R_{ku} values – were observed for the Ni-free SS sample, describing a surface with more pronounced and dominant peaks compared to valleys. This emphasizes the advantage of 3D analysis in capturing morphological features that may be missed by 2D-only profiling.

Two additional parameters, texture aspect ratio (S_{tr}) and surface slope (S_{dq}) proved to be valuable for monitoring and further describing surface changes. When interpreted alongside other roughness parameters, they provide additional insight into the nature and complexity of surface alterations. For example, in sample 1 (NiTi archwire, Fig. 1), where the lowest roughness was recorded at pH 6.6, a higher S_{tr} value compared to the control and pH 5.5 conditions indicates a more uniform distribution of newly formed peaks. At the same time, a decrease in S_{dq} indicates that these peaks formed more uniformly and gradually, probably because the surface depressions were gradually filled. This combination of higher isotropy (S_{tr}) and lower root mean square slope (S_{dq}) reflects a smoother and more homogeneously modified surface, which may affect the functional performance of the material.

Briefly, among the tested archwires, the NiTi alloy shows moderate surface roughness and a balanced peak-to-valley distribution, with pH 6.6 causing more pronounced changes than pH 5.5, especially in peak distribution and surface smoothing. The coated NiTi archwire has lower roughness values and a more uniform surface, but responds differently to pH changes, with the treated samples showing increased roughness and peak height. The SS archwire is more resistant to changes at a pH of 5.5 than at 6.6. In contrast, the Ni-free SS alloy appears to be more sensitive at a pH of 5.5, at which significant deformation and internal structural changes occur. The CoCr archwire exhibits minimal roughness in the untreated state, but undergoes significant surface changes at pH 6.6, including pick thickening and ion release. Finally, the TiMo alloy shows severe structural deformation at pH 5.5, similar to sample Ni-free SS.

In addition to AFM, SEM/EDX was used to further investigate the surface morphology and elemental composition of the archwires. SEM analysis provides complementary information by revealing surface defects, microstructural features, and changes in elemental distribution that are not always detectable with AFM alone.[4,33] Deams *et al.* have shown in their study that each wire has its own SEM surface characteristics. There are large differences in the type and number of surface defects between the different samples in the initial state (parent), but also in the wires modified under test conditions.[4] Similar results are also confirmed in this study. Each wire exhibited unique morphological characteristics in the untreated state, which were further altered by exposure to artificial saliva at different pH values. Changes included surface cracking, increased roughness, formation of oxide layers and redistribution of elements, especially in Ni-free SS (at both tested pH), SS (at pH 6.6) and CoCr wires (at pH 5.5). NiTi and TiMo wires showed relatively stable surfaces, while coated NiTi wires exhibited smoother morphology and less element loss, indicating a protective effect of the coating. These results provide crucial insight into the corrosion behavior and surface deterioration of orthodontic archwires under simulated intraoral conditions. The observed morphological changes – such as surface cracks, increased roughness and the formation of oxide layers – are consistent with previous studies highlighting the susceptibility of orthodontic alloys to corrosion in an acidic environment.[4,16] NiTi wires, known for their corrosion resistance, maintained a balanced Ni : Ti ratio and minimal surface damage, which is consistent with the findings of Konda *et al.*[35] Coated NiTi wires exhibited smoother surfaces and lower elemental losses, suggesting that esthetic coatings could provide protective benefits, although the presence of unexpected elements (*e.g.*, S, Al, Ca) in the EDX spectra could indicate environmental interactions or contamination. SS wires showed moderate corrosion with visible surface cracks and reduced Fe and Cr content at a pH of 5.5, indicating localized corrosion and disruption of the passive layer, as confirmed in studies mapping elemental loss in SS orthodontic appliances.[36] Ni-free SS wires were most affected by the acidic conditions and exhibited pronounced surface degradation and high oxygen content, raising concerns about their long-term mechanical integrity and biocompatibility. CoCr wires maintained their surface integrity better at pH 6.6, and showed signs of selective dissolution and degradation of the passive layer at pH 5.5, consistent with SEM corrosion studies.[4,16] TiMo wires exhibited deep striations and local oxidation at both tested pH values, but retained relatively stable elemental composition, supporting their potential as a hypoallergenic alternative with favorable corrosion profiles.[35]

Obtained SEM/EDX findings complement the AFM results, confirming that surface roughness and chemical degradation are closely linked. The degree of oxidation and elemental loss observed in SEM/EDX correlates with increased roughness parameters (R_y, S_q, W_a), particularly in Ni-free SS and TiMo wires at pH 5.5.

PCA revealed that the measured variables group into three functional categories: topographical parameters, chemical composition, and mechanical surface performance. Factor 1 primarily reflects chemical influences, while factor 2 is

associated with surface texture. The PCA scatter plot shows that control samples cluster closely, indicating consistent baseline properties, whereas treated samples diverge depending on pH and material type. Alloys such as CoCr, TiMo, and Ni-free SS exhibit greater sensitivity to pH changes, with more pronounced shifts in both chemical and topographical characteristics. So, PCA further supported the differentiation of archwire types based on topographical and chemical parameters.

Obtained results emphasize the importance of selecting materials for orthodontic wires based on their corrosion resistance and surface stability. Materials such as NiTi and TiMo may offer superior performance in variable pH environments and reduce the risk of ion release, mechanical failure and undesirable biological reactions. Conversely, Ni-free SS and CoCr alloys need to be carefully considered, especially in patients with acidic oral conditions or metal sensitivities.

The formation of oxide layers, surface cracks, and elemental redistribution may influence the mechanical performance of the wires, including their flexibility, frictional behavior, and ion release potential. Clinically, this underscores the importance of selecting archwire materials based on their resistance to corrosion and surface degradation, especially in patients with poor oral hygiene or acidic oral environments. These findings are especially relevant given increasingly stringent global regulatory requirements that emphasize standardized characterization, biomaterial safety, and controlled ion release – trends consistent with recent analyses of regulatory directions in the biomedical field.[47] Future research should include *in vivo* analyses and longer exposure periods to better simulate clinical conditions. Additionally, exploring the effects of protein-rich media and mechanical stress could further clarify the mechanisms of archwire degradation.

Conclusions

The findings of this study provide a clearer understanding of how commonly used orthodontic archwires respond to clinically relevant acidic conditions. Using both AFM and SEM/EDX, distinct material-specific patterns were identified: NiTi, coated NiTi, and TiMo alloys maintained stable surface profiles and showed minimal elemental loss, while Ni-free stainless steel and CoCr archwires exhibited pronounced surface degradation and reduced chemical stability.

These insights highlight the importance of thorough surface and chemical characterization when evaluating the corrosion resistance and structural reliability of orthodontic materials. They also reinforce the clinical relevance of careful material selection, especially for patients with acidic oral conditions or metal sensitivities, in accordance with current regulatory expectations for safety, quality, and transparent material characterization.

Beyond direct clinical applications, by supporting the development of safer orthodontic devices, reducing the risk of adverse reactions, and promoting more durable and cost-effective treatments, these results contribute to broader community well-being. Improved material standards ultimately benefit not only patients and clinicians but also manufacturers, regulatory bodies, and public health efforts to ensure the safety and reliability of medical devices.

This research ultimately supports more evidence-based decisions in orthodontic practice and contributes to the development of safer, more durable archwires designed to meet the challenges of the oral environment.

Author contributions

Conceptualization, G. Č. J.; methodology, Z. J. O., I. J. B, K. K, J. A. J. and A. R.; software, G. Č. J.; formal analysis, Z. J. O., I. J. B. and K. K.; investigation, G. Č. J.; resources G. Č. J.; data curation, G. Č. J.; writing—original draft preparation, G. Č. J.; writing—review and editing, G. Č. J.; visualization, G. Č. J.; supervision, G. Č. J.; project administration, G. Č. J.; funding acquisition, G. Č. J.

Conflicts of interest

There are no conflicts to declare.

Data availability

Data for this article, [named: Dataset for manuscript: Topographical characterization of orthodontic archwires] are available at Zenodo at https://www.doi.org/10.5281/zenodo.17701982.

Acknowledgements

The work was carried out with the financial support of the University of Rijeka, projects by experienced scientists: Determination of the harmful effects of metal ions eluted from orthodontic materials (uniri-iskusni-biomed-23-102).

References

1 R. Kotha, R. K. Alla, S. Mohammed and R. Ravi, *Trends Biomater. Artif. Organs*, 2014, **18**, 32–36.
2 A. Fróis, A. C. Santos and C. S. Louro, *Metals*, 2023, **13**, 1955.
3 V. D'Antò, R. Rongo, G. Ametrano, G. Spagnuolo, P. Manzo, R. Martina, S. Paduano and R. Valletta, *Angle Orthod.*, 2012, **82**, 922–928.
4 J. Daems, J.-P. Celis and G. Willems, *Eur. J. Orthod.*, 2009, **31**, 260–265.
5 L. Vezenkov and J. Guillen, *Ann. Orthod. Periodontics Spec.*, 2025, **5**, 114–129.
6 M. Mikulewicz, P. Suski, O. Tokarczuk, M. Warzyńska-Maciejewska, P. Pohl and B. Tokarczuk, *Molecules*, 2024, **29**, 5685.
7 M. Petković Didović, I. Jelovica Badovinac, Ž. Fiket, J. Žigon, M. Rinčić Mlinarić and G. Čanadi Jurešić, *Materials*, 2023, **16**, 4156.
8 Z. Jusufi Osmani, P. Tariba Knežević, D. Vučinić, J. Alimani Jakupi, A. A. Reka, M. Can, K. Kara and V. Katić, *Materials*, 2024, **17**, 5254.

9 V. Kovac, B. Poljsak, M. Bergant, J. Scancar, U. Mezeg and J. Primozic, *Coatings*, 2022, **12**, 190.
10 E. S. A. Aziz, S. B. A. Syed Bakhtiar Ariffin, S. D. Sinniah and H. B. Said Gulam Khan, *Clin. Investig. Orthod.*, 2025, **84**, 136–143.
11 C.-O. A. Olsson and D. Landolt, *Electrochim. Acta*, 2003, **48**, 1093–1104.
12 D. D. Macdonald, *Electrochim. Acta*, 2011, **56**, 1761–1772.
13 M. A. Blesa, *Chemical Dissolution of Metal Oxides*, CRC Press, Milton, 1st edn, 2018.
14 P. Marcus and V. Maurice, in *Materials Science and Technology*, ed. R. W. Cahn, P. Haasen and E. J. Kramer, Wiley, 1st edn, 2013.
15 P. M. Natishan and W. E. O'Grady, *J. Electrochem. Soc.*, 2014, **161**, C421–C432.
16 K. House, F. Sernetz, D. Dymock, J. R. Sandy and A. J. Ireland, *Am. J. Orthod. Dentofacial Orthop.*, 2008, **133**, 584–592.
17 T. Eliades and A. E. Athanasiou, *Angle Orthod.*, 2002, **72**, 222–237.
18 A. S. Toloei, V. Stoilov and D. O. Northwood, *Simultaneous Effect of Surface Roughness and Passivity on Corrosion Resistance of Metals*, València, Spain, 2015, pp. 355–367, https://www.witpress.com/elibrary/wit-transactions-on-engineering-sciences/90/33289.
19 J. Bącela, M. B. Łabowska, J. Detyna, A. Zięty and I. Michalak, *Materials*, 2020, **13**, 3257.
20 J. Liang, K. Xu, S. Arora, J. E. Laaser and S. K. Fullerton-Shirey, *Materials*, 2020, **13**, 1089.
21 J. L. Xu, T. Lai and J. M. Luo, *Prog. Org. Coat.*, 2019, **137**, 105271.
22 M. C. De Amorim, S. Da Rocha Gomes, B. P. Da Silva, I. V. Aoki and R. T. Basting, *J. Bio Tribo Corros.*, 2022, **8**, 22.
23 A. A. Aboalnaga and A. M. E. Shahawi, *BMC Oral Health*, 2023, **23**, 816.
24 E. S. Gadelmawla, M. M. Koura, T. M. A. Maksoud, I. M. Elewa and H. H. Soliman, *J. Mater. Process. Technol.*, 2002, **123**, 133–145.
25 M. McDonough, P. Perov, W. Johnson, and S. Radojev, *Undergraduate Theses and Capstone Projects*, Suffolk University, 2020.
26 *DIN EN ISO 4287:2010-07*, 2010.
27 *ISO 25178-2:2021*, 2021.
28 M. Shamohammadi, E. Hormozi, M. Moradinezhad, M. Moradi, M. Skini and V. Rakhshan, *Int. Orthod.*, 2019, **17**, 60–72.
29 R. Wang, Y. Li, T. Xiao, L. Cong, Y. Ling, Z. Lu, C. Fukushima, I. Tsuchitori and M. Bazzaoui, *Sci. Rep.*, 2019, **9**, 13094.
30 S. Ryu, B. Lim, E. J. Kwak, G. Lee, S. Choi and K. Park, *Scanning*, 2015, **37**, 414–421.
31 G.-J. Lee, K.-H. Park, Y.-G. Park and H.-K. Park, *Micron*, 2010, **41**, 775–782.
32 M. P. Didović, K. Kara, I. J. Badovinac, R. Peter, Ž. Fiket, I. Suman, T. Kowalkowski and G. Č. Jurešić, *J. Mater. Sci.: Mater. Med.*, 2025, **36**, 74.
33 K. Akhtar, S. A. Khan, S. B. Khan and A. M. Asiri, in *Handbook of Materials Characterization*, ed. S. K. Sharma, Springer International Publishing, Cham, 2018, pp. 113–145.
34 F. Amini, V. Rakhshan, M. Pousti, H. Rahimi, M. Shariati and B. Aghamohamadi, *Korean J. Orthod.*, 2012, **42**, 129.
35 P. Konda, R. Kamble and A. Kumar, *J. Indian Orthod. Soc.*, 2013, **47**, 16–20.
36 T. Gedrange, *Med. Sci. Monit.*, 2014, **20**, 860–865.
37 V. Kararia, P. Jain, S. Chaudhary and N. Kararia, *Contemp. Clin. Dent.*, 2015, **6**, 44.
38 I. Uysal, B. Yilmaz, A. O. Atilla and Z. Evis, *Eng. Sci. Technol. Int. J.*, 2022, **36**, 101277.
39 K. Kaczmarek, A. Leniart, B. Lapinska, S. Skrzypek and M. Lukomska-Szymanska, *Materials*, 2021, **14**, 2624.
40 M. D. Ferrer, S. Pérez, A. L. Lopez, J. L. Sanz, M. Melo, C. Llena and A. Mira, *Int. J. Environ. Res. Public Health*, 2021, **18**, 6049.
41 J. C. Wataha, *J. Prosthet. Dent.*, 2000, **83**, 223–234.
42 M. Skliar and V. S. Chernyshev, *JoVE*, 2019, 59254.
43 M. Hugenschmidt, K. Adrion, A. Marx, E. Müller and D. Gerthsen, *Microsc. Microanal.*, 2023, **29**, 219–234.
44 M. A. Gravina, C. Canavarro, C. N. Elias, M. das Graças Afonso Miranda Chaves, I. H. V. P. Brunharo and C. C. A. Quintão, *Dent. Press J. Orthod.*, 2014, **19**, 69–76.
45 T. Eliades, *Eur. J. Orthod.*, 2000, **22**, 317–326.
46 F. L. Gewers, G. R. Ferreira, H. F. D. Arruda, F. N. Silva, C. H. Comin, D. R. Amancio and L. D. F. Costa, *ACM Comput. Surv.*, 2022, **54**, 1–34.
47 N. Verma and S. Arora, *Pharmaceutics*, 2025, **17**, 990.